Effect of pH on the Final Connectivity Distribution of the Silicon Atoms in the Stöber Particles

KANGTAEK LEE*

Department of Chemical Engineering, Yonsei University, 134 Shinchon-dong, Seodaemun-gu, Seoul, 120-749, Korea

ktlee@yonsei.ac.kr

ALON V. McCORMICK*

Department of Chemical Engineering and Materials Science, University of Minnesota, Minneapolis, MN 55455, USA

mccormic@cems.umn.edu

Abstract. Using ^{29}Si MAS-NMR we investigate the effect of pH on the final connectivity distribution of the silicon atoms in the Stöber particles. Our data suggest that the fraction of the silicon atoms that are fully-connected decreases as the ammonia concentration is increased. This suggests a *more* negative first shell substitution effect in the precipitated phase (liquid droplet) if condensation reactions are irreversible. A simple model is developed to describe the condensation kinetics in the precipitated phase, and the results support the negative first shell substitution effect. These findings challenge the notion of a positive first shell substitution effect in alkaline conditions.

Keywords: Stöber particles, ^{29}Si MAS-NMR, pH, first shell substitution effect, condensation kinetics

1. Introduction

Recently monodispersely-sized spherical colloids in sub-micron range are attracting interests in the areas of pharmaceuticals and electronics as well as fine ceramics and coatings [1–3]. A well-known system to produce such colloids is the Stöber process in which tetraethoxysilane (TEOS) is hydrolyzed by using the base catalyst to produce monodispersely-sized silica colloids [4]. The excellent monodispersity in the size of silica colloids made the Stöber process the most extensively studied system to date [5–9]. It is not yet well understood, however, what is responsible for such an easy production of monodispersely-sized silica colloids in the Stöber process.

*To whom all correspondence should be addressed.

Several researchers have used both solution and solid-state ^{29}Si-NMR to study the connectivity distribution of the silicon atoms in silica gel and particles [8–12]. When TEOS is hydrolyzed under acidic conditions, it was found that there was more Q_3 than Q_4 even after gelation [10–12] (here Q represents a quadra-functional silicon site, and the subscript i represents the number of siloxane bridges connected to the silicon atom). On the other hand, when a base was used as a catalyst in the Stöber process, van Blaaderen and Kentgens [8] reported that silica particles were made of more Q_4 than Q_3 ($\sim$65% Q_4, $\sim$30% Q_3, and $\sim$5% Q_2). However, they did not systematically change the initial solution composition of the system to understand the effect of initial pH on particle structure.

To rationalize structural features of the reaction products of TEOS in acidic vs. basic condition, two

contrasting condensation reaction pathways have been suggested. Both are based on a first-shell-substitution effect (FSSE), in which the condensation reaction rate of the functional groups depends only on its nearest neighbors. In the first pathway, with a negative FSSE, the condensation rates decrease as the functional groups become more highly connected [13–16]. In the alternative pathway, with a positive FSSE, the condensation rates increase as the reacting sites become more highly connected [17].

In acidic TEOS systems (pH < 3), transparent gels with a fractal dimension near two form [18, 19]. Many researchers have ascribed low fractal dimension to a negative FSSE [18, 19]. The fact that there is more Q_3 than Q_4 in the final gel supports this explanation [10–12]. Independent kinetic studies have confirmed that a negative FSSE operates in many acidic systems [13–16].

In contrast, in basic TEOS systems (pH > 10) particles with a fractal dimension near three are formed [18, 19]. To explain high fractal dimension, it has been suggested that there may be a strong positive FSSE [17]. This might also explain the absence of dimer and larger oligomers by solution ^{29}Si-NMR. However, Kallala et al. [17] did not consider precipitation, which may be responsible for the nucleation [9], in their model.

Brinker and Assink [20] proposed a simple functional form for the irreversible condensation rate constants in order to test the FSSE. They assumed that the condensation rate constant ($k_{i,j}$) for Q_i and Q_j could be represented by two parameters (i.e., dimerization rate constant $k_{0,0}$ and R):

$$k_{i,j} = k_{0,0} R^{i+j} \qquad (1)$$

where R is an adjustable parameter that accounts for the change in the condensation kinetics with the extent of condensation. If R is greater than 1, there should be a positive FSSE since k_{ij} increases with the higher i and j, while there is a negative FSSE if R is less than 1. This is shown in Fig. 1 where the calculated connectivity distributions for two different R values (0.5 and 1.5) are compared with that without a FSSE, i.e. $R = 1$ (we will present this reaction scheme later). When there is a negative FSSE ($R = 0.5$, Fig. 1(a)), one should expect lower $[Q_4]$ and higher $[Q_3]$ at high conversion than when there is no FSSE. However, with a positive FSSE ($R = 1.5$, Fig. 2(b)) the opposite (higher $[Q_4]$ and lower $[Q_3]$) is true.
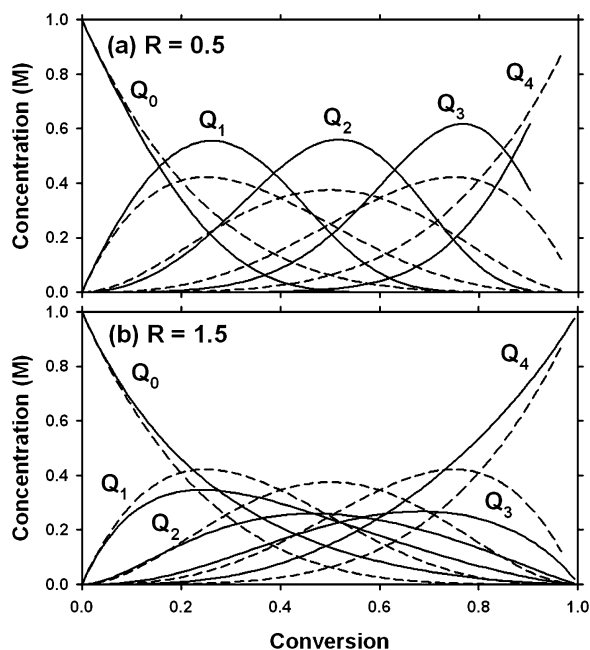

Figure 1. Evolution of Q_i's with (a) a negative first-shell-substitution effect ($R = 0.5$), and with (b) a positive first-shell-substitution effect ($R = 1.5$); $[Q_0]_0 = 1.0$ M; $[Q_i]_0$'s $= 0.0$ M for $i = 1, 2, 3, 4$; $k_{0,0} = 0.1$ l/mol·hr; and the dotted lines are drawn without a FSSE ($R = 1$).

In our previous work [9], we have suggested that in the Stöber process the doubly-hydrolyzed monomer precipitates, which is followed by the formation of primary particles. These primary particles are colloidally unstable, so they aggregate until stable particles are made. However, the condensation reaction kinetics in the precipitated phase (probably inside liquid droplets) before the formation of primary particles is not yet understood. In alkaline TEOS systems, there might be localized reactions inside liquid droplet, which could explain the high fractal dimension of the final particles even with a negative FSSE.

In this paper, we will vary the initial ammonia concentrations in the Stöber process to change the initial pH, and use ^{29}Si MAS-NMR to estimate the connectivity distribution of the silicon atoms in the final silica particles. We will also use a simple model based on Brinker and Assink's work [20] to test whether there is a positive or negative FSSE in alkaline TEOS systems.

2. Experimental

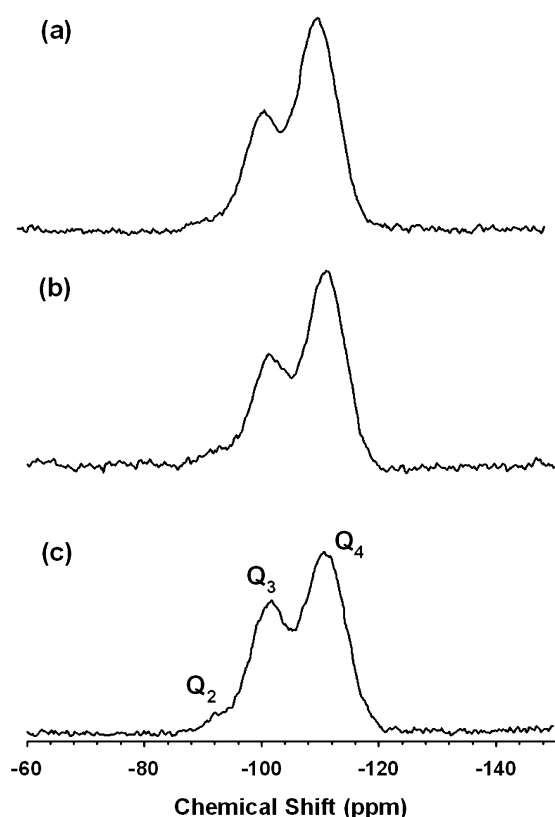Tetraethoxysilane (TEOS, 98% purity, Aldrich); deionized, distilled and filtered H_2O; a standard 4.96 N

Figure 2. ^{29}Si MAS-NMR spectra at three different ammonia concentrations; $[TEOS]_0 = 0.15$ M, and $[H_2O]_0 = 8.8$ M; (a) 0.1 M NH$_3$, (b) 0.3 M NH$_3$, and (c) 1.0 M NH$_3$.

ammonium hydroxide solution (Aldrich) were dissolved in ethanol (Aaper alcohol and chemical co.) so that the final compositions were 0.15 M TEOS:8.8M H$_2$O:0.1, 0.3, and 1.0 M NH$_3$. After a week, the particles produced were collected by centrifugation or by reverse-osmosis, and they were air-dried before the ^{29}Si MAS-NMR experiments. For reverse osmosis, stirred cell from Amicon with an ultrafiltration membrane (50,000 MW cut-off) was used and pressure up to 20 psi was applied.

For ^{29}Si MAS-NMR, 400 MHz spectrometer from ChemMagnetics with 5 mm sample rotor was used. The spectral frequency for silicon was 79.5 MHz, and the 90° pulse width was 7.0 μs. Though it would have shortened the acquisition time, we chose to forgo cross-polarization to ensure quantitative results. The delay time was 300 s, which was taken from van Blaaderen et al.'s experiment [8], and 192 FID's were accumulated for each spectrum. Deconvolution was performed using Spinsight software by adjusting the peak frequency, lineshape, width, and height to get the best fit.[1]

3. Results and Discussion

3.1. ^{29}Si MAS-NMR Results

^{29}Si MAS-NMR spectra at three different ammonia concentrations are shown in Fig. 2. Table 1 shows the individual concentration of different Q_i species and the conversions. Conversion is defined as the fraction of the alkoxyl bonds that are reacted to form siloxane bonds. As the ammonia concentration is increased (higher pH), the fraction of Q_3 increases while that of Q_4 decreases, and the fraction of Q_2 remains virtually the same. Note that the conversions in all three systems are close to 90%, which is consistent with the previous reports by van Blaaderen and Kentgens [8]. If there is a crossover from a negative to a positive FSSE as pH increases (i.e., stronger positive FSSE at higher pH [17]) and condensation reactions are irreversible, the fraction of Q_4 should increase as the ammonia concentration is increased, but this is not true in the present study. This suggests that there might be a negative FSSE inside liquid droplets, contrary to the previous models [17]. Next, we will develop a simple model which is similar to the Brinker and Assink's model [20] to test whether there really is a negative FSSE even in alkaline system.

Table 1. The connectivity distribution of the silicon atoms in the Stöber particles at different ammonia concentrations ([TEOS] = 0.15 M, and [H$_2$O] = 8.8 M).

[NH$_3$] (M)	Q_0 (%)	Q_1 (%)	Q_2 (%)	Q_3 (%)	Q_4 (%)	Conversion (%)
0.1	0.0	0.0	3.2	30.1	66.7	90.9
0.3	0.0	0.0	3.4	33.1	63.5	89.9
1.0	0.0	0.0	3.7	39.8	56.5	88.2

3.2. Modeling of Condensation Kinetics

First, we make the following assumptions:

(1) As soon as the doubly-hydrolyzed monomer (Q_0^2) precipitates to produce liquid droplets, it becomes fully hydrolyzed to form Q_0, i.e., hydrolysis in liquid droplet is instantaneous (note that this is a hydrophilic or water-rich phase). Here the superscript denotes the number of hydroxyl bonds on a silicon atom. Thus, there is no need to include hydrolysis inside liquid droplets in the model (Q_0^2 can be considered as Q_0 in liquid droplets).

(2) Condensation reactions inside liquid droplets are irreversible.

(3) Because the model is so rough and we cannot fit the individual rate constants, we will use the expression suggested by Brinker and Assink [20]. The condensation rate constant for Q_i and Q_j are approximated in the following three ways:
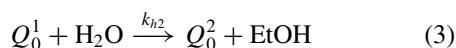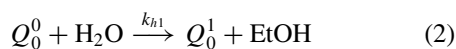
    (a) $k_{i,j} = k_{0,0}\, R^{i+j}$
    (b) $k_{i,j} = k_{0,0}\, R^{\max(i,j)}$
    (c) $k_{i,j} = k_{0,0}\, R^{\min(i,j)}$

    where $k_{0,0}$ is a dimerization rate constant. Note that the case (c) was consistent with the experimental results in acidic TEOS systems [13].
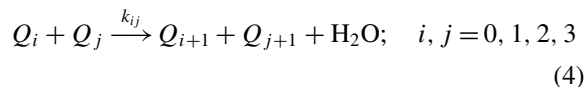
(4) The condensation reaction between particles caused by aggregation is not considered separately. The reaction scheme includes the condensation reactions which follow aggregation.

(5) Cyclization is neglected. This surely occurs, but Ng and McCormick have shown that its neglect causes the underestimation of the negative FSSE (i.e., even higher R will be predicted) [22].

(6) The change in [Si] inside liquid droplets as a result of precipitation is not explicitly modeled. This factor is lumped into the bimolecular rate constants in the scheme, so they should not be considered true homogeneous rate constants.

The following reaction scheme (a site-based model) is considered:

In solution:

$$Q_0^0 + H_2O \xrightarrow{k_{h1}} Q_0^1 + EtOH \qquad (2)$$

$$Q_0^1 + H_2O \xrightarrow{k_{h2}} Q_0^2 + EtOH \qquad (3)$$

In liquid droplets:

$$Q_i + Q_j \xrightarrow{k_{ij}} Q_{i+1} + Q_{j+1} + H_2O; \quad i, j = 0, 1, 2, 3 \qquad (4)$$

The rate expressions can be simplified as follows:

$$\frac{d[Q_0^0]}{dt} = -k_{h1}[Q_0^0][H_2O] \qquad (5)$$

$$\frac{d[Q_0^1]}{dt} = k_{h1}[Q_0^0][H_2O] - k_{h2}[Q_0^1][H_2O] \qquad (6)$$

$$\frac{d[Q_i]}{dt} = \sum_{j=0}^{3} k_{i-1,j}[Q_{i-1}][Q_j] - \sum_{j=0}^{3} k_{i,j}[Q_i][Q_j] + \delta_{i,0}k_{h2}[Q_0^1][H_2O] \qquad (7)$$

In Eq. (7), $i = 0, 1, 2, 3, 4$ and $k_{i,j} \neq 0$ only if $0 \leq i,\, j \leq 3$, and $\delta_{i,j} = 0$ if $i \neq j$. We solve the set of the above coupled differential equations to fit the Q-distribution at the final conversion (Table 1) by optimizing $k_{0,0}$ and R. Here, we used the values for k_{h1} and k_{h2} from ref. [9] (Table 2). When Brinker and Assink applied a similar method to acidic TEOS system, they found that R was $\sim$0.35, confirming a negative FSSE [20]. Table 3 shows the optimized $k_{0,0}$ and R values for three different ammonia concentrations. Figure 3 shows the evolution of Q_i's with conversion using the optimized parameters.[2]

In all three cases, the dimerization rate constant increases as the ammonia concentration is increased, and the R value is virtually the same. Note that R is always LESS THAN 1! This suggests that there still might be a negative FSSE in alkaline condition, though may not be as severe as in acidic condition where R is $\sim$0.35. Probably, this is due to the severe steric hindrance inside liquid droplets after precipitation. However, because of many assumptions made in this model (for instance, the condensation reactions are assumed irreversible), it is still necessary to develop a more comprehensive model.

Table 2. Hydrolysis rate constants used in the model ([TEOS] = 0.15 M, and [H_2O] = 8.8 M).

[NH_3] (M)	k_{h1} (l/mol·hr)	k_{h2} (l/mol·hr)
0.1	2.3×10^{-2}	1.6×10^{-1}
0.3	9.6×10^{-2}	6.7×10^{-1}
1.0	3.1×10^{-1}	2.1

Table 3. Optimized $k_{0,0}$ and R at different ammonia concentrations ([TEOS] = 0.15 M, and [H_2O] = 8.8 M).

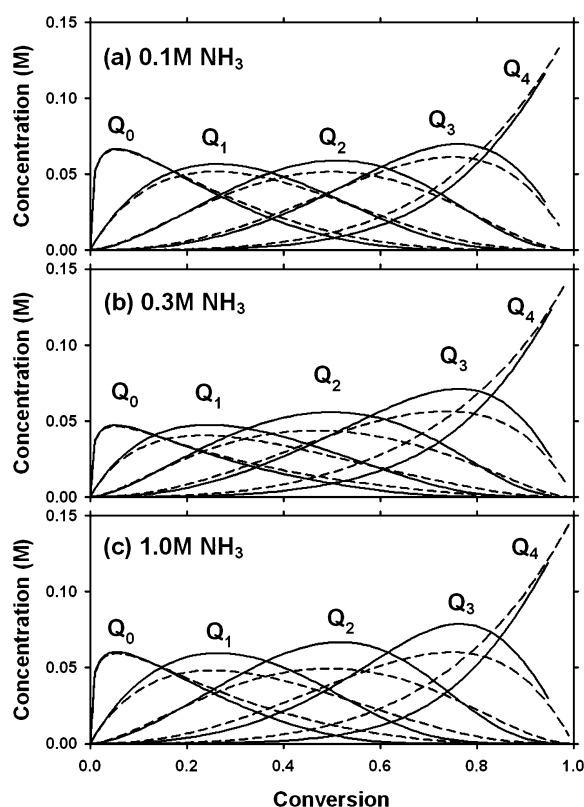| [NH_3] (M)	$k_{0,0}$ (l/mol·hr)	R
(a) $k_{i,j} = k_{0,0}R^{i+j}$		
0.1	0.12	0.86
0.3	1.34	0.80
1.0	2.23	0.71
(b) $k_{i,j} = k_{0,0}R^{\max(i,j)}$		
0.1	0.84	0.59
0.3	1.1	0.61
1.0	2.1	0.45
(c) $k_{i,j} = k_{0,0}R^{\min(i,j)}$		
0.1	0.60	0.64
0.3	0.98	0.67
1.0	1.83	0.51

Figure 3. Evolution of Q_i's from a model at three different ammonia concentrations; [TEOS]_0 = 0.15 M, and [H_2O]_0 = 8.8 M, and the dotted lines are drawn without a FSSE; (a) 0.1 M NH_3, (b) 0.3 M NH_3, and (c) 1.0 M NH_3.

4. Summary

^{29}Si MAS-NMR is used to study the effect of pH on the final connectivity distribution of the silicon atoms in the Stöber particles. As the pH is increased, the fraction of fully-connected silicon atoms decreases, while the fraction of triply-connected silicon atoms increases. This is not consistent with the previous model (i.e., with a positive first shell substitution effect), but suggests a negative first-shell-substitution effect. A simple model also suggests that there might be a negative first shell substitution effect in alkaline conditions as in acidic conditions. However, one would still need to consider reversibility of condensation reactions to confirm this result.

Acknowledgments

Notes

1. In deconvolution, 100% Gaussian lines are found to fit the peaks most closely. This suggests that these particles are amorphous [21].
2. The optimized curves were virtually the same for all three cases.

References

1. Y.A. Vlasvo, X.-Z. Bo, J.C. Sturm, and D.J. Norris, Nature **414**, 289 (2001).
2. H. Goto, T. Isobe, and M. Senna, J. Nanoparticle Res. **1**, 205 (1999).
3. Y.J. Kim and L.F. Francis, J. Am. Ceram. Soc. **76**, 737 (1993).
4. W. Stöber, A. Fink, and E. Bohn, J. Colloid Interface Sci. **26**, 62 (1968).
5. T. Matsoukas and E. Gulari, J. Colloid Interface Sci. **132**, 13 (1989).
6. G.H. Bogush and C.F. Zukoski, J. Colloid Interface Sci. **142**, 1 (1991).
7. M.T. Harris, Ultrafine Precursor Powders by Homogeneous Precipitation and Electrodispersion, Ph.D. dissertation, Univ. of Tennessee, 1992.
8. A. van Blaaderen and A.P.M. Kentgens, J. Non-Cryst. Solids **149**, 161 (1992).
9. K. Lee, J.-L. Look, M.T. Harris, and A.V. McCormick, J. Colloid. Interface Sci. **194**, 78 (1997).

10. J. Sanchez, Kinetics and Models of Silicon Alkoxide Polymerization, Ph.D. Dissertation, University of Minnesota, 1994.

11. L. Malier, F. Devreux, F. Chaput, J.P. Boilot, and M.A.V. Axelos, J. Non-Cryst. Solids **147/148**, 686 (1992).

12. L. Malier, F. Devreux, F. Chaput, and J.P. Boilot, in *Chemical Processing of Advanced Materials*, edited by L.L. Hench and J.K. West (John Wiley & Sons, Inc., 1992), p. 59.

13. J. Sanchez, S.E. Rankin, and A.V. McCormick, Ind. Eng. Chem. Res. **35**, 117 (1996).

14. J.C. Pouxviel and J.P. Boilot, J. Non-Cryst. Solids **94**, 374 (1987).

15. C.J. Brinker and G.W. Scherer, *Sol-Gel Science* (Academic Press, San Diego, 1990).

16. D.H. Doughty, R.A. Assink, and B.D. Kay, Adv. Chem. **224**, 241 (1990).

17. M. Kallala, R. Jullien, and B. Cabane, J. Phys. II France **2**, 7 (1992).

18. D.W. Schaefer and K.D. Keefer, in *Better Ceramics Through Chemistry*, edited by C.J. Brinker, D.E. Clark, and D.R. Ulrich (Material Research Society, Pittsburgh, 1984), p. 1.

19. C.J. Brinker, K.D. Keefer, D.W. Schaefer, R.A. Assink, B.D. Kay, and C.S. Ashley, J. Non-Cryst. Solids **63**, 45 (1984).

20. C.J. Brinker and R.A. Assink, J. Non-Cryst. Solids **111**, 48 (1989).

21. K.A.M. Thakur, R.T. Kean, J.M. Zupfer, N.U. Buehler, M.A. Doscotch, and E.J. Munson, Macromolecules **29**, 8844 (1996).

22. L.V. Ng and A.V. McCormick, J. Phys. Chem. **100**, 12517 (1996).